



Universiteit  
Leiden  
The Netherlands

## Plasmonic enhancement of one-photon- and two-photon-excited single-molecule fluorescence by single gold nanorods

Zhang, W.

### Citation

Zhang, W. (2018, June 27). *Plasmonic enhancement of one-photon- and two-photon-excited single-molecule fluorescence by single gold nanorods*. *Casimir PhD Series*. Retrieved from <https://hdl.handle.net/1887/62864>

Version: Not Applicable (or Unknown)

License: [Licence agreement concerning inclusion of doctoral thesis in the Institutional Repository of the University of Leiden](#)

Downloaded from: <https://hdl.handle.net/1887/62864>

**Note:** To cite this publication please use the final published version (if applicable).

Cover Page



Universiteit Leiden



The handle <http://hdl.handle.net/1887/62864> holds various files of this Leiden University dissertation

**Author:** Zhang, Weichun

**Title:** Plasmonic enhancement of one-photon- and two-photon-excited single-molecule fluorescence by single gold nanorods

**Date:** 2018-06-28

# 6

## **Plasmonic enhancement of molecular two-photon-excited fluorescence by individual gold nanorods**

*In this chapter, we demonstrate two-photon-excited fluorescence enhancement for an ensemble of Rhodamine 6G molecules. Our results show that due to the presence of a single gold nanorod, fluorescence of the molecules in the near field is enhanced, on average, by a factor of about 4,500 at best. The enhancement shows a strong dependence on the plasmon resonance of the nanorods, and is independent of the excitation laser intensity if the excitation is under the reshaping threshold of the nanorods.*

## 6.1. Introduction

In Chapter 5, we have demonstrated large enhancement of two-photon-excited luminescence for single semiconductor quantum dots. This was possible largely thanks to the high two-photon absorption cross-sections of quantum dots. Organic dye molecules, however, have typically 3 orders of magnitude lower two-photon absorption cross-sections than quantum dots [1–3]. The sizes of molecules are much smaller ( $\sim 1 - 3$  nm). This features a major advantage as fluorescent probes over bulky quantum dots, whose size can easily reach 20 nm with the chemical coatings for better biocompatibility. Smaller size leads lower effects on the motion, localization and interactions of tagged objects, which is highly desired for fluorescence correlation spectroscopy, single-molecule imaging, *etc.* For these reasons, it is highly desirable to enhance the two-photon-excited fluorescence of dye molecules.

The two-photon-excited fluorescence enhancement of fluorescent dyes has already been measured a number of times in ensemble, where under different conditions different enhancement factors were found [4–6]. In this chapter, we systematically studied the two-photon fluorescence enhancement of Rhodamine 6G by single gold nanorods. Our results show that molecules near a gold nanorod can be enhanced by a factor of 4,500, averaged over all the molecules in the near-field.

## 6.2. Experimental section

**Materials.** Spectroscopy grade methanol (99.9%) was purchased from Alfa Aesar. Rhodamine 6G was purchased from Eastman. Gold nanorods were from Nanopartz Inc. The longitudinal surface plasmon resonance (LSPR) of the nanorods was 770 nm as obtained from the UV-Vis spectrum (Fig. S6.1). Their average dimensions were  $38 \text{ nm} \times 118 \text{ nm}$  as obtained from the transmission electron microscopy image provided by the manufacturer. Gold nanorods were immobilized onto a microscope coverslip with a spin-coating method described elsewhere [7, 8]. The coverslip was mounted in a home-made sample holder, where the sample solutions can be added for further optical measurements. A second cover glass was placed immediately on top to prevent the evaporation of methanol.

**Two-photon microscopy.** Single-particle spectroscopy was performed on a same optical setup as described in Chapter 4. Briefly, we used a mode-locked titanium-sapphire laser (775 nm wavelength and 220 fs pulse width, Mira 900, Coherent) with circular polarization to excite fluorescence from the molecules in a home-built confocal microscope equipped with time-correlated single-photon counting (TCSPC) electronics (TimeHarp 200, PicoQuant GmbH, Berlin). A 612-nm shortpass filter was used in the detection path to reject most of the two-photon-excited luminescence signal from the gold nanorods. The plasmon resonance of each gold nanorod is determined by measuring the one-photon-excited photoluminescence spectrum in clean methanol excited by a 532-nm continuous-wave laser prior to the two-photon measurements. Apart from more commonly used scattering spectra, photoluminescence spectra have been proven and used as an alternative method of measuring the plasmon resonances [9, 10].

In order to characterize two-photon fluorescence enhancement, emission signals from three different experimental conditions have to be compared (see Fig. 6.1). (a) The femtosecond laser was focused on a single gold nanorod in clean methanol. Strong two-photon-

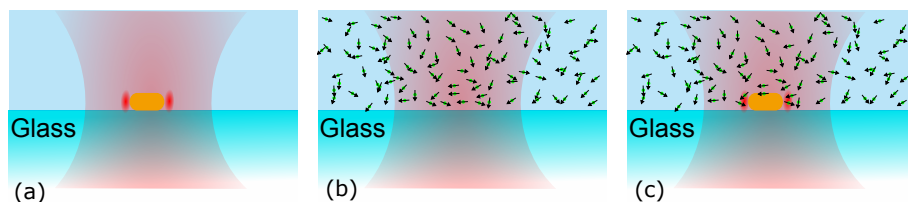


Figure 6.1: **Three measurements required to characterize the ensemble enhancement of Rhodamine 6G fluorescence.** (a) A single immobilized nanorod immersed in methanol. (b) Rhodamine 6G solution without a nanorod. (c) The same nanorod as in (a) immersed in the Rhodamine 6G solution.

excited luminescence signal from the nanorod was observed as a result of the strong two-photon absorption due to the resonant excitation of the surface plasmon [11–13], despite that only a small fraction of the emission was detected due to the 612-nm shortpass filter. See Chapter 4 for the optical characterizations of two-photon luminescence from gold nanorods. (b) Methanol was replaced by a solution of 5.34 mM Rhodamine 6G dissolved in methanol and the laser was focused on the solution/glass interface. (c) The laser was then parked on the same nanorod as in (a) but immersed in Rhodamine 6G solution. The laser power was the same for the three conditions. Time traces were recorded in time-tagged-time-resolved mode and further analyzed with SymPhoTime software (PicoQuant GmbH, Berlin).

### 6.3. Results and discussion

Figure 6.2(a) shows the time traces from the three measurements shown in Fig. 6.1 with an average laser power of  $1.5 \mu\text{W}$ . Figure 6.2(b) shows the one-photon-excited luminescence spectrum of the nanorod shown in (a). A Lorentzian fit to the spectrum yields a plasmon resonance at  $761.6 \pm 0.3 \text{ nm}$  and a full width at half maximum (FWHM) of  $51.3 \pm 0.7 \text{ nm}$ . The narrow Lorentzian lineshape confirms that it is from a single gold nanorod. The spectrum has been normalized by the spectral response of the optical setup (see Chapter 2). The time traces show no higher fluctuations than the photon noise. Firstly, the laser power was kept below that required for photothermal reshaping of a gold nanorod [14–16] (see Chapter 5 for the discussion on nanorod reshaping), so the luminescence emission is stable. Secondly, fluorescence fluctuation due to molecules diffusing in and out of the confocal volume or the optical near field in the vicinity of the gold nanorod is not visible because of the high concentration of molecules. We measured the size of the focal volume by a separate experiment to be  $0.09 \pm 0.01 \text{ fL}$  (See Fig. S4.2 in Chapter 4). We estimate  $\sim 144,000$  molecules in the upper half of the focal volume for a dye concentration of 5.34 mM. The size of the near field is  $\sim 1000$  times smaller than the half focal volume (denoted "far field" hereafter). The near field accommodates  $\sim 144$  molecules. We therefore do not expect any significant fluctuation of fluorescence in the time traces.

Excluding the dark count rate ( $64 \pm 2 \text{ counts/s}$ ), the count rates from nanorod luminescence and unenhanced molecules in the far field were  $778 \pm 11 \text{ counts/s}$  and  $1820 \pm 19 \text{ counts/s}$ , respectively; the count rate from the nanorod in the Rhodamine 6G solution was  $7140 \pm 37 \text{ counts/s}$ , which was higher than the sum of nanorod luminescence and

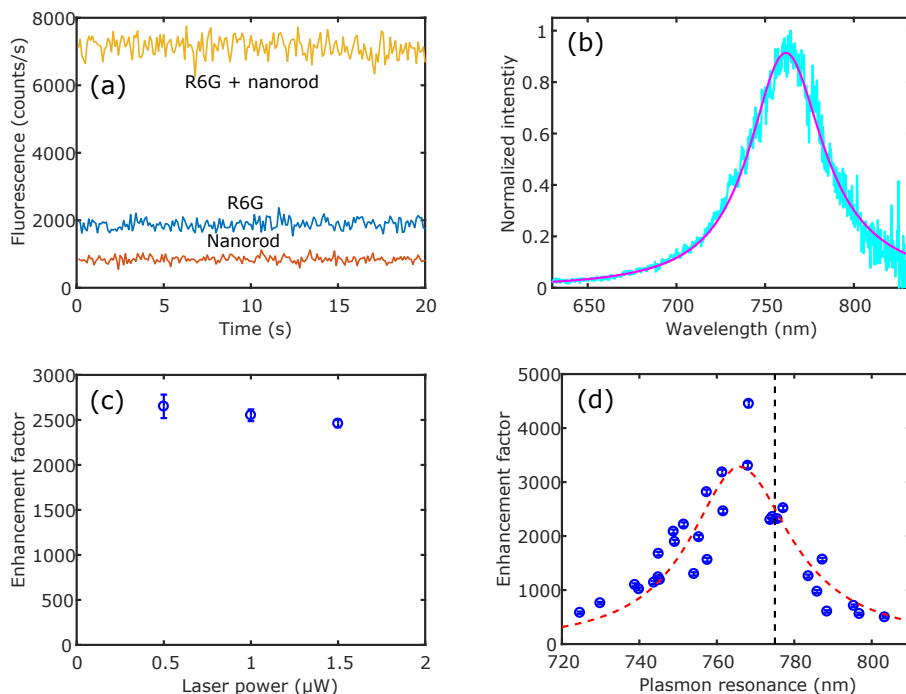


Figure 6.2: **Experimental results.** (a) Fluorescent time traces recorded on a nanorod in methanol (orange), Rhodamine 6G solution without a nanorod (blue) and a nanorod in Rhodamine 6G solution (yellow). (b) The one-photon-excited luminescence spectrum of the nanorod shown in (a). The magenta solid curve represents a Lorentzian fit to the spectrum, which yields a plasmon resonance wavelength of  $761.6 \pm 0.3$  nm and a full width at half maximum (FWHM) of  $51.3 \pm 0.7$  nm. (c) Fluorescence enhancement factor as a function of the excitation laser power. (d) The blue circles represent the measured fluorescence enhancement factor as a function of the plasmon resonance of the single gold nanorods. The error bars are smaller than the circles representing the data points. The black dashed line shows the wavelength of the excitation laser (775 nm). The red dashed curve is a Lorentzian fit to the data, which yields a FWHM of  $31.8 \pm 5.6$  nm.

molecule fluorescence when measured separately. (The mean values and uncertainties of photon counts were estimated by fitting the interphoton times to mono-exponentials without binning the photons.) The extra signal ( $4478 \pm 43$  counts/s) was from the molecules in the near field whose two-photon fluorescence was strongly enhanced by the gold nanorod. In other words, although the molecules in the plasmonic hotspot are 1000 times fewer in number than in the far field, they contribute to  $2.46 \pm 0.05$  times higher count rate than all the molecules in the far field. This corresponds to an average enhancement factor of  $2460 \pm 50$ . We note this enhancement factor is a rough estimate since the volume of the near field is not well-defined.

It was previously reported that the high temperature of the electron gas (thousands of K) upon femtosecond excitation leads to the transient broadening of the plasmon resonance [17]. This broadening appears during the exciting pulse and might potentially hinder the efficiency of plasmonic effects, such as fluorescence enhancement. If this is the case, fluo-

rescence enhancement should decrease with increasing excitation intensity. To address this point, we measured the fluorescence enhancement of Rhodamine 6G with varying average laser powers and the results are shown in Fig. 6.2(c). Measurements on four more different nanorods are presented in Fig. S6.4. We see that the enhancement factor does not show significant decrease with increasing power, suggesting that two-photon fluorescence enhancement is not notably affected by the plasmon broadening.

Fluorescence enhancement depends on the plasmon resonance wavelength of individual nanorods. With the plasmon resonance closer to the excitation wavelength, a nanorod creates a stronger near field intensity, hence higher fluorescence enhancement. We repeated the enhancement experiment for 29 more single nanorods and plotted the measured fluorescence enhancement factors in Fig. 6.2(d), which shows a clear plasmon resonance dependence. A maximum enhancement factor of 4,500 was achieved by a nanorod with a plasmon resonance wavelength of 768 nm, which is very close to the laser wavelength (775 nm). We fitted the enhancement factors to a Lorentzian function and obtained a full width at half maximum (FWHM) of  $31.8 \pm 5.6$  nm, which is narrower than the typical linewidth of the plasmon resonance of a single gold nanorod ( $\sim 50$  nm, see Fig. 6.2(b)). The sharper dependence is consistent with the nonlinear nature of the two-photon-excited fluorescence enhancement.

## 6.4. Conclusion

By measuring on the same nanorod in different situations, we clearly and convincingly demonstrated two-photon-excited fluorescence enhancement for Rhodamine 6G by single gold nanorods. The enhancement strongly depends on the position of the plasmon resonances of the nanorods, and is independent of the excitation laser intensity if the excitation is under the reshaping threshold. We deduced a molecular enhancement factor of 4,500 averaged over the molecules in the near field of a nanorod in the best case.

## 6.5. Supporting information

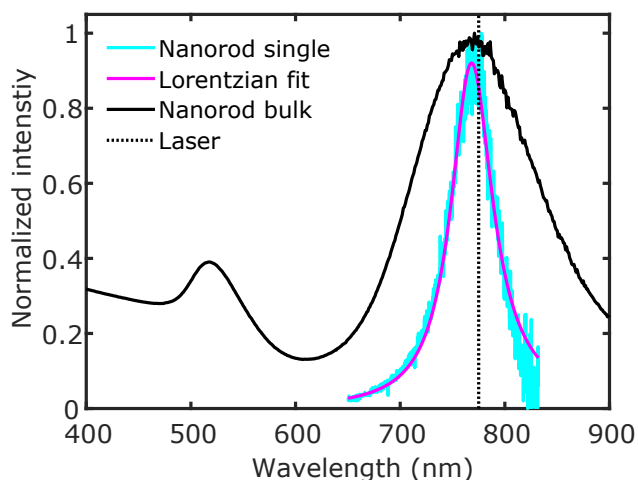


Figure S6.1: **Spectra of gold nanorods.** The black line shows the bulk extinction spectrum of gold nanorods used in this work dispersed in water. The extinction maximum was observed at 771 nm. The broad extinction band stems from the size distribution of nanorods in the suspension. The cyan curve shows the one-photon-excited photoluminescence spectrum of a single gold nanorod. The spectrum is corrected for the wavelength-dependence collecting efficiency of the setup and fitted with a Lorentzian line shape (magenta), yielding a resonance wavelength of  $768.2 \pm 0.3$  nm. The wavelength of the excitation laser (775 nm) is represented by the dashed vertical lines in the plots.

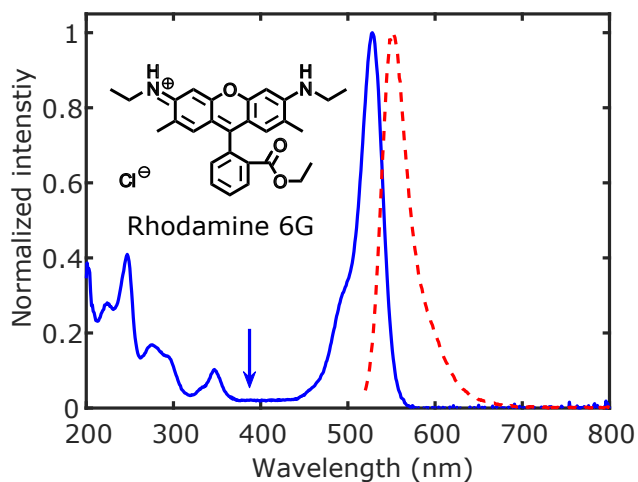


Figure S6.2: **Spectra of Rhodamine 6G.** Absorption and emission spectra of a solution of Rhodamine 6G in methanol are shown as the blue solid line and red dashed line, respectively ( $\lambda_{\text{max-abs}} \sim 528$  nm,  $\lambda_{\text{max-em}} \sim 552$  nm). The blue vertical arrow indicates the wavelength corresponding to the total energy of two excitation photons. Inset: chemical structure of Rhodamine 6G.



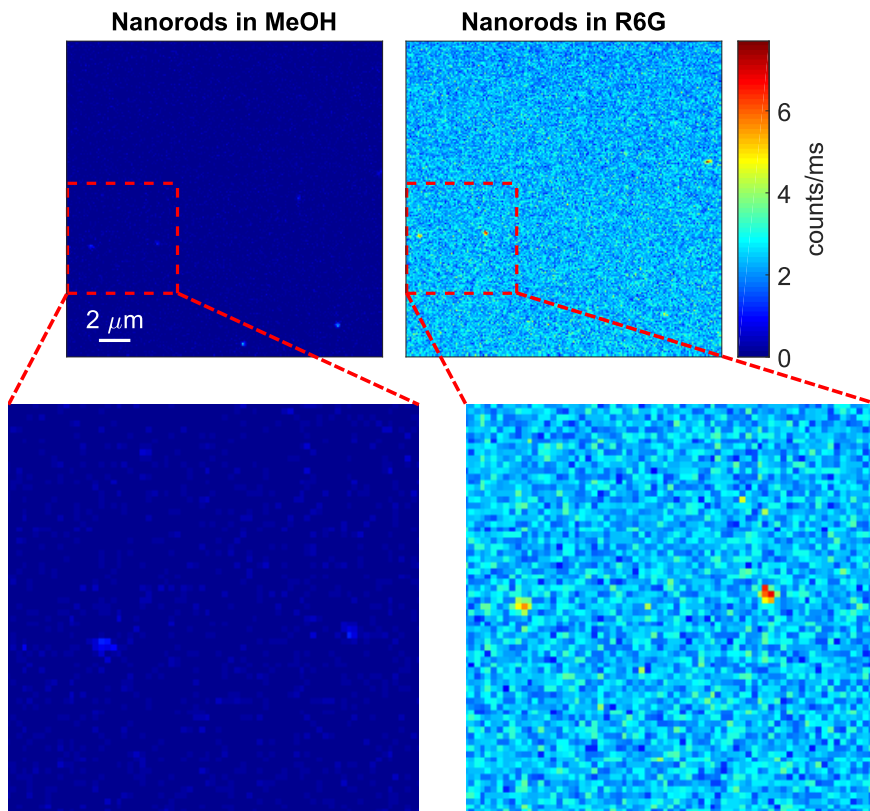


Figure S6.3: **Fluorescence images ( $20\ \mu\text{m} \times 20\ \mu\text{m}$ ) of gold nanorods in clean methanol (left) and Rhodamine 6G (right).** The spots in the left image come from the two-photon-excited luminescence gold nanorods. After methanol was replaced by 5.34 mM Rhodamine 6G, the same nanorods shown in the left image were identified despite of the small drift. The images consist of  $200 \times 200$  pixels with an integration time of 10 ms/pixel. An area of  $7\ \mu\text{m} \times 7\ \mu\text{m}$  containing two nanorods is expanded. The excitation was the femtosecond laser (circularly polarized) with an average power of  $1.5\ \mu\text{W}$  at the sample. A 612-nm short-pass filter was used for the images. Intensity enhancement is already visible by comparing of the brightness of the spots for the same nanorods in different images, but to measure the enhancement with more accuracy, we have to record time traces both on and outside nanorods.

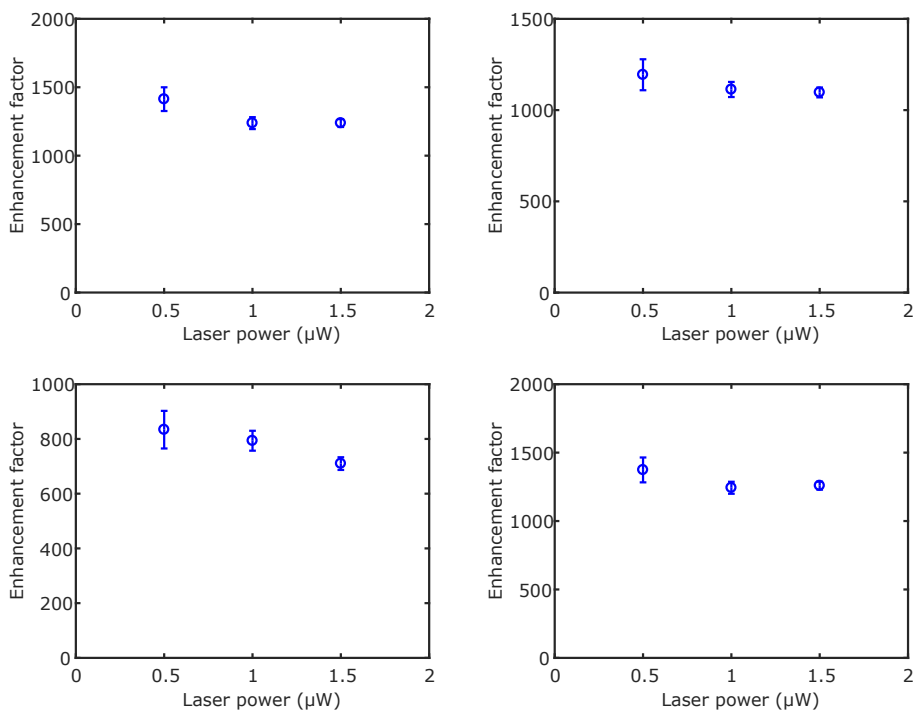


Figure S6.4: Power-dependent measurements of the enhancement factors for four more nanorods.

## References

- [1] M. A. Albota, C. Xu, and W. W. Webb, *Two-photon fluorescence excitation cross sections of biomolecular probes from 690 to 960 nm*, *Applied Optics* **37**, 7352 (1998).
- [2] C. Xu and W. W. Webb, *Measurement of two-photon excitation cross sections of molecular fluorophores with data from 690 to 1050 nm*, *JOSA B* **13**, 481 (1996).
- [3] D. R. Larson, W. R. Zipfel, R. M. Williams, S. W. Clark, M. P. Bruchez, F. W. Wise, and W. W. Webb, *Water-soluble quantum dots for multiphoton fluorescence imaging in vivo*, *Science* **300**, 1434 (2003).
- [4] T. Zhao, K. Yu, L. Li, T. Zhang, Z. Guan, N. Gao, P. Yuan, S. Li, S. Q. Yao, Q.-H. Xu, and G. Q. Xu, *Gold nanorod enhanced two-photon excitation fluorescence of photosensitizers for two-photon imaging and photodynamic therapy*, *ACS Applied Materials & Interfaces* **6**, 2700 (2014).
- [5] S. T. Sivapalan, J. H. Vella, T. K. Yang, M. J. Dalton, R. N. Swiger, J. E. Haley, T. M. Cooper, A. M. Urbas, L.-S. Tan, and C. J. Murphy, *Plasmonic enhancement of the two photon absorption cross section of an organic chromophore using polyelectrolyte-coated gold nanorods*, *Langmuir* **28**, 9147 (2012).
- [6] I. Cohanoschi, S. Yao, K. D. Belfield, and F. E. Hernández, *Effect of the concentration of organic dyes on their surface plasmon enhanced two-photon absorption cross section using activated au nanoparticles*, *Journal of Applied Physics* **101**, 086112 (2007).
- [7] H. Yuan, S. Khatua, P. Zijlstra, M. Yorulmaz, and M. Orrit, *Thousand-fold enhancement of single-molecule fluorescence near a single gold nanorod*, *Angewandte Chemie International Edition* **52**, 1217 (2013).
- [8] W. Zhang, M. Caldarola, B. Pradhan, and M. Orrit, *Gold nanorod enhanced fluorescence enables single-molecule electrochemistry of methylene blue*, *Angewandte Chemie International Edition* **56**, 3566 (2017).
- [9] M. Yorulmaz, S. Khatua, P. Zijlstra, A. Gaiduk, and M. Orrit, *Luminescence quantum yield of single gold nanorods*, *Nano Letters* **12**, 4385 (2012).
- [10] A. Carattino, S. Khatua, and M. Orrit, *In situ tuning of gold nanorod plasmon through oxidative cyanide etching*, *Physical Chemistry Chemical Physics* **18**, 15619 (2016).
- [11] C. Molinaro, Y. El Harfouch, E. Palleau, F. Eloi, S. Marguet, L. Douillard, F. Charra, and C. Fiorini-Debuisschert, *Two-photon luminescence of single colloidal gold nanorods: Revealing the origin of plasmon relaxation in small nanocrystals*, *The Journal of Physical Chemistry C* **120**, 23136 (2016).
- [12] N. Gao, Y. Chen, L. Li, Z. Guan, T. Zhao, N. Zhou, P. Yuan, S. Q. Yao, and Q.-H. Xu, *Shape-dependent two-photon photoluminescence of single gold nanoparticles*, *The Journal of Physical Chemistry C* **118**, 13904 (2014).

- 
- [13] P. Zijlstra, J. W. Chon, and M. Gu, *Five-dimensional optical recording mediated by surface plasmons in gold nanorods*, *Nature* **459**, 410 (2009).
- [14] W. Albrecht, T.-S. Deng, B. Goris, M. A. van Huis, S. Bals, and A. van Blaaderen, *Single particle deformation and analysis of silica-coated gold nanorods before and after femtosecond laser pulse excitation*, *Nano Letters* **16**, 1818 (2016).
- [15] P. Zijlstra, J. W. Chon, and M. Gu, *White light scattering spectroscopy and electron microscopy of laser induced melting in single gold nanorods*, *Physical Chemistry Chemical Physics* **11**, 5915 (2009).
- [16] A. B. Taylor, A. M. Siddiquee, and J. W. M. Chon, *Below melting point photothermal reshaping of single gold nanorods driven by surface diffusion*, *ACS Nano* **8**, 12071 (2014).
- [17] S. Link and M. A. El-Sayed, *Spectral properties and relaxation dynamics of surface plasmon electronic oscillations in gold and silver nanodots and nanorods*, *The Journal of Physical Chemistry B* **103**, 8410 (1999).